THE JOURNAL OF BIOLOGICAL CHEMISTRY VOL. 289, NO. 38, pp. 26618–26629, September 19, 2014

A Novel Non-agonist Peroxisome Proliferator-activated Receptor γ (PPARγ) Ligand UHC1 Blocks PPARγ Phosphorylation by Cyclin-dependent Kinase 5 (CDK5) and Improves Insulin Sensitivity*

Received for publication, March 25, 2014, and in revised form, July 28, 2014 Published, JBC Papers in Press, August 6, 2014, DOI 10.1074/jbc.M114.566794

Sun-Sil Choi[‡], Eun Sun Kim[‡], Minseob Koh[§], Soo-Jin Lee[‡], Donghyun Lim[¶], Yong Ryoul Yang[‡], Hyun-Jun Jang[‡], Kyung-ah Seo[‖], Sang-Hyun Min[‖], In Hee Lee[1], Seung Bum Park[§¶2], Pann-Ghill Suh[‡], and Jang Hyun Choi[‡3]**

*From the [‡]Department of Biological Science, Ulsan National Institute of Science and Technology, Ulsan 689-798, Korea, the [§]Department of Chemistry, Seoul National University, Seoul 151-747, Korea, the [¶]New Drug Development Center, Daegu-Gyeongbuk Medical Innovation Foundation, 80 Cheombok-ro, Dong-gu, Daegu 701-310, Korea, the [‖]Department of Biophysics and Chemical Biology/Bio-MAX Institute, Seoul National University, Seoul 151-747, Korea, and the **Department of Medical Chemistry, Hyundai Pharm Co., Ltd., Suwon, Gyonggi 443-270, Korea*

Background: PPARγ ligands can be used in numerous metabolic syndromes.
Results: A novel non-agonist PPARγ ligand, UHC1 exhibited great beneficial effects on glucose metabolism and anti-inflammatory response.
Conclusion: UHC1 shows anti-diabetic action by blocking CDK5-mediated PPARγ phosphorylation.
Significance: UHC1 can be a novel therapeutic agent for use in type 2 diabetes and related metabolic disorders.

Thiazolidinedione class of anti-diabetic drugs which are known as peroxisome proliferator-activated receptor γ (PPARγ) ligands have been used to treat metabolic disorders, but thiazolidinediones can also cause several severe side effects, including congestive heart failure, fluid retention, and weight gain. In this study, we describe a novel synthetic PPARγ ligand UNIST HYUNDAI Compound 1 (UHC1) that binds tightly to PPARγ without the classical agonism and which blocks cyclin-dependent kinase 5 (CDK5)-mediated PPARγ phosphorylation. We modified the non-agonist PPARγ ligand SR1664 chemically to improve its solubility and then developed a novel PPARγ ligand, UHC1. According to our docking simulation, UHC1 occupied the ligand-binding site of PPARγ with a higher docking score than SR1664. In addition, UHC1 more potently blocked CDK5-mediated PPARγ phosphorylation at Ser-273. Surprisingly, UHC1 treatment effectively ameliorated the inflammatory response both *in vitro* and in high-fat diet-fed mice. Furthermore, UHC1 treatment dramatically improved insulin sensitivity in high-fat diet-fed mice without causing fluid retention and weight gain. Taken together, compared with SR1664, UHC1 exhibited greater beneficial effects on glucose and lipid metabolism by blocking CDK5-mediated PPARγ phosphorylation, and these data indicate that UHC1 could be a novel therapeutic agent for use in type 2 diabetes and related metabolic disorders.

Peroxisome proliferator-activated receptor γ (PPARγ)[4] is a member of the nuclear receptor family of ligand-activated transcription factors (1, 2). It is highly expressed in adipose tissue and regulates diverse biological functions, including adipocyte differentiation, lipid metabolism, and inflammation (3). There are two isoforms of PPARγ, PPARγ1 and PPARγ2, which are generated by alternative promoter use. PPARγ2, which contains an additional 30 amino acids at the N terminus compared with PPARγ1, is expressed predominantly in adipose tissue, whereas PPARγ1 is expressed ubiquitously (4). Biological ligands for PPARγ are yet to be identified, but PPARγ can be activated by various fatty acids and their metabolites, as well as by the thiazolidinedione (TZD) class of anti-diabetic drugs, which includes rosiglitazone and pioglitazone (5, 6).

PPARγ activation requires the stabilization of helix 12 or AF-2 (activation function-2) region after the binding of a ligand to the ligand binding domain (LBD) of PPARγ (7, 8). For example, TZDs bind directly to the PPARγ LBD and activate the transcription of PPARγ target genes that play roles in a variety of metabolic pathways (6). PPARγ can also be activated by partial agonists. Some selective PPARγ modulators bind to the PPARγ LBD and increase PPARγ transcriptional activity (9). Although the structural mechanism behind the activation of PPARγ by these molecules is poorly understood, it may stabilize other regions in the ligand binding pocket such as the helix 3 region (10). Nevertheless, these molecules have similar glucose-lowering and anti-diabetic effects as full agonists, with reduced side effects such as weight gain and fluid retention (11, 12). These results strongly suggest that PPARγ agonism is not

* This work was supported by Basic Science Research Program through the National Research Foundation of Korea funded by Ministry of Education, Science and Technology Grant NRF-2012R1A1A1015407 (to S.-S. C., E. S. K., and J. H. C.), and the 2012 Research Fund of Ulsan National Institute of Science and Technology (to S.-J. L.).
[1] Supported by a Hyundai Pharm Research Grant.
[2] Supported by Bio and Medical Technology Development Program Grant 2012M3A9C4048780 and Basic Research Laboratory Grant 2010-0019766.
[3] To whom correspondence should be addressed: Dept. of Biological Sciences, Ulsan National Institute of Science and Technology, Ulsan 689-798, Korea. Tel.: 82-52-217-2543; Fax: 82-52-217-5219; E-mail: janghchoi@unist.ac.kr.

[4] The abbreviations used are: PPARγ, peroxisome proliferator-activated receptor γ; LBD, ligand binding domain; CDK5, cyclin-dependent kinase 5; HFD, high-fat diet; MGL, monoacylglycerol lipase; HSL, hormone-sensitive lipase; qPCR, quantitative PCR.

correlated directly with anti-diabetic action. Recently, we demonstrated that the phosphorylation of PPARγ by cyclin-dependent kinase 5 (CDK5) did not alter its adipogenic activity, but dysregulated a specific set of genes with roles in obesity and diabetes (13, 14). Importantly, the non-agonist PPARγ ligand SR1664 blocked PPARγ phosphorylation and exerted potent anti-diabetic activity, but with fewer side effects such as fluid retention, bone fractures, and weight gain (14). These results indicate that it may be possible to develop novel anti-diabetic drugs that target PPARγ. However, SR1664 has poor chemical properties, including its pharmacokinetics and solubility; therefore, we modified SR1664 to improve these parameters.

In the current study, we developed a novel non-agonist PPARγ ligand (UHC1) that blocked CDK5-mediated PPARγ phosphorylation, avoided classical PPARγ agonism, and bound strongly to the LBD of PPARγ. A biophysical analysis revealed that UHC1 bound directly to the LBD of PPARγ without activating its transcriptional activity. UHC1 did not enhance adipogenesis or adipogenic gene expression in 3T3-L1 cells. Interestingly, UHC1 significantly inhibited the inflammatory responses in both 3T3-L1 adipocytes and Raw264.7 macrophages. In addition, UHC1 improved insulin sensitivity without the common side effects of TZDs, including weight gain and fluid retention, in mice fed a high-fat diet (HFD). Taken together, these data indicate that non-agonist PPARγ ligands could be used to treat type 2 diabetes and that UHC1 is a potent therapeutic agent for diabetes.

EXPERIMENTAL PROCEDURES

Cell Culture—3T3-L1, HEK-293, and Raw264.7 cells were obtained from ATCC and cultured in Dulbecco's modified Eagle's medium with 10% fetal bovine serum. FLAG-PPARγ and FLAG-PPARγ S273A were subcloned into pMSCV-puro retroviral vector (Agilent Tech.). Adipocyte differentiation of 3T3-L1 was performed described previously (13, 14). 3T3-L1 adipocytes or Raw264.7 cells were preincubated with PPARγ agonists for 24 h and treated with TNF-α (10 ng/ml) for 3 h or LPS (100 ng/ml) for 6 h, respectively. All chemicals for cell culture were obtained from Sigma unless otherwise indicated.

UHC1 (4′-((2,3-Dimethyl-5-(pyridin-3-ylmethylcarbamoyl)-1H-indol-1-yl)methyl)biphenyl-2-carboxylic Acid)—A mixture of tert-butyl 4′-((2,3-dimethyl-5-(pyridin-3-ylmethylcarbamoyl)-1*H*-indol-1-yl)methyl)biphenyl-2-carboxylate (88 mg, 0.18 mmol/l) in TFA/dichloromethane (DCM) (3 ml, 30%) was stirred for 2 h. The completion of the reaction was monitored by TLC. The solvent was removed to obtain the crude that was purified by column chromatography to obtain the title compound (^{1}H NMR (400 MHz, dimethyl sulfoxide-d_6): δ 8.99 (t, J = 5.6 Hz, 1H), 8.65 (s, 1H), 8.55 (d, J = 4.8 Hz, 1H), 8.10 (s, 1H), 7.93 (d, J = 7.6 Hz, 1H), 7.70–7.64 (m, 2H), 7.55–7.41 (m, 4H), 7.32 (d, J = 7.6 Hz, 1H), 7.24 (d, J = 7.6 Hz, 2H), 7.00 (d, J = 7.6 Hz, 2H), 5.54 (s, 2H), 4.56 (d, J = 5.6 Hz, 2H), 2.32 (s, 3H), 2.27 (s, 3H) (see Fig. 1*a*)).

In Vitro Kinase and Binding Assay—Active CDK5/p35 kinase were purchased from Millipore. *In vitro* CDK kinase assay was performed according to the manufacturer's instructions (Cell Signaling Technology). Briefly, 0.5 μg of recombinant PPARγ (Cayman Chemicals) were incubated with active CDK kinase in kinase assay buffer (25 mmol/liter Tris-HCl, pH 7.5, 5 mmol/liter β-glycerophosphate, 2 mmol/liter DTT, 0.1 mmol/liter Na_3VO_4, 10 mmol/liter $MgCl_2$) containing 20 μmol/liter ATP for 15 min at 30 °C. Positive control for assay, purified retinoblastoma protein (Rb; Cell Signaling Technology) was used. UHC1 was pre-incubated with substrates for 10 min, and the assay was performed. Phosphorylation of substrates after SDS-PAGE was analyzed with anti-CDK substrate antibody to detect phospho-Ser in a KSPXK motif, which is the consensus motif for CDK substrate proteins (Cell Signaling Technology) (13). LanthaScreen TR-FRET PPARγ competitive binding assay was performed according to the manufacturer's instructions (Invitrogen).

In Silico Binding Simulation—The binding pose was predicted by docking simulation using the Discovery Studio 1.7® program. PPARγ ligand-binding pockets were defined from receptor cavities, and the LigandFit module implemented in the Receptor-Ligand Interaction protocol was used for detailed calculations. X-ray crystal structure of PPARγ ligand binding domain (Protein Data Bank code 2HFP) was used in the docking simulation and the subsequent structural analysis with the Discovery Studio Visualizer 3.0® program (Accelrys Software, Inc.).

Surface Plasmon Resonance—The dissociation constant of compounds toward His-PPARγ-LBD was determined by surface plasmon resonance spectroscopy using a Biacore T100 instrument (GE Healthcare). The surface carboxyl group of CM5 sensor chip was activated with a mixture of 1-ethyl-3-(3-dimethylaminopropyl)-carbodiimide and *N*-hydroxysuccinimide in flow cells 1 and 2 to generate the reactive succinimide ester on the surface of sensor chip. Human PPARγ-LBDs (20 mmol/liter HEPES, 1 mmol/liter TCEP, pH 8.0) were then immobilized on the flow cell 2 via amide bond formation with succinimide ester on the surface of sensor chip. The remaining succinimide ester on flow cells 1 and 2 was quenched by injecting 1 mol/liter ethanolamine-HCl (pH 8.0). Phosphate buffered saline (PBS, 137 mmol/liter NaCl, 2.7 mmol/liter KCl, 10 mmol/liter Na_2HPO_4, 2 mmol/liter KH_2PO_4, pH 7.4) was used as the running buffer throughout the immobilization process. After immobilization, various concentrations of the ligands (SR1664, 100 nmol/liter to 1 μmol/liter; UHC1, 300 nmol/liter to 2 μmol/liter) were injected for 60 s at a flow rate of 30 μl/min, and dissociation from the sensor surface was monitored for 360 s at the same flow rate. A 20 mmol/liter HEPES buffer (pH 8.0) containing 5% (w/v) dimethyl sulfoxide, 150 mmol/liter NaCl, 1 mmol/liter EDTA, and 0.005% (w/v) P20 was used as the running buffer. The binding events were measured at 25 °C. Data were analyzed using the Biacore T100 Evaluation software (GE Healthcare). Final sensorgrams were obtained by eliminating responses from flow cell 1 and the buffer-only control. The dissociation constant (K_D) was calculated by fitting the sensorgrams to the 1:1 binding model.

Immunoprecipitation and Immunoblotting—HEK-293 cells expressing PPARγ were treated with TNF-α (50 ng/ml), and total cell lysates were incubated with FLAG M2 agarose (Sigma) at 4 °C. Immunoprecipitates or total cell or tissue lysates were analyzed with phospho-specific antibody against PPARγ Ser-273 (13) or anti-PPARγ antibody (Santa Cruz Biotechnology).

Reporter Gene Assay—HEK-293 cells were transfected with pDR-1 luciferase reporter plasmid, PPARγ, RXRα, and pRL-*Renilla* using Lipofectamine 2000 (Invitrogen). Following an

TABLE 1
Primer sequences used in this work

Gene	Forward primer	Reverse primer
ap2	AAGGTGAAGAGCATCATAACCCT	TCACGCCTTTCATAACACATTCC
C/EBPα	CAAGAACAGCAACGAGTACCG	GTCACTGGTCAACTCCAGCAC
Glut4	GTGACTGGAACACTGGTCCTA	CCAGCCACGTTGCATTGTAG
Fasn	GCTGGCATTCGTGATGGAGTCGT	AGGCCACCAGTGATGATGTAACTCT
LPL	GGGAGTTTGGCTCCAGAGTTT	TGTGTCTTCAGGGGTCCTTAG
PPARγ	GCATGGTGCCTTCGCTGA	TGGCATCTCTGTGTCAACCATG
Adiponectin	TGTTCCTCTTAATCCTGCCCA	CCAACCTGCACAAGTTCCCTT
Adipsin	CATGCTCGGCCCTACATGG	CACAGAGTCGTCATCCGTCAC
IL-6	TAGTCCTTCCTACCCCAATTTCC	TTGGTCCTTAGCCACTCCTTC
TNF-α	CCCTCACACTCAGATCATCTTCT	GCTACGACGTGGGCTACAG
IL-1β	AAATACCTGTGGCCTTGGGC	CTTGGGATCCACACTCTCCAG
MCP-1	TTAAAAACCTGGATCGGAACCAA	GCATTAGCTTCAGATTTACGGGT
Arginase	ATGGAAGAGACCTTCAGCTAC	GCTGTCTTCCCAAGAGTTGGG
IL-10	CATGGCCCAGAAATCAAGGA	GGAGAAATCGATGACAGCGC
MGL	ATGATGTCTGCCAGAGAACC	ATCACAGATTTCAGCAACCTTA
HSL	GCTGGGCTGTCAAGCACTGT	GTAACTGGGTAGGCTGCCAT
ATGL	ACACCAGCATCCAGTTCAA	GGTTCAGTAGGCCATTCCTC
Cycp2f2	GTCGGTGTTCACGGTGTACC	AAAGTTCCGCAGGATTTGGAC
Rarres2	GCCTGGCCTGCATTAAAATGG	CTTGCTTCAGAATTGGGCAGT
Selenbp1	ATGGCTACAAAATGCACAAAGTG	CCTGTGTTCCGGTAAATGCAG
Car3	TGACAGGTCTATGCTGAGGGG	CAGCGTATTTTACTCCGTCCAC
Peg10	TGCTTGCACAGAGCTACAGTC	AGTTTGGGATAGGGGCTGCT
Cidec	ATGGACTACGCCATGAAGTCT	CGGTGCTAACACGACAGGG
Cd24a	GTTGCACCGTTTCCCGGTAA	CCCCTCTGGTGGTAGCGTTA
Acyl	CAGCCAAGGCAATTTCAGAGC	CTCGACGTTTGATTAACTGGTCT
Nr1d2	TGAACGCAGGAGGTGTGATTG	GAGGACTGGAAGCTATTCTCAGA
Ddx17	TCTTCAGCCAACAATCCCAATC	GGCTCTATCGGTTTCACTACG
Aplp2	GTGGTGGAAGACCGTGACTAC	TCGGGGGAACTTTAACATCGT
Nr3c1	AGCTCCCCCTGGTAGAGAC	GGTGAAGACGCAGAAACCTTG
Rybp	CGACCAGGCCAAAAAGACAAG	CACATCGCAGATGCTGCATT
Txnip	TCTTTTGAGGTGGTCTTCAACG	GCTTTGACTCGGGTAACTTCACA
Nr1d1	TACATTGGCTCTAGTGGCTCC	CAGTAGGTGATGGTGGGAAGTA

overnight transfection, the cells were treated with rosiglitazone or UHC1 for 24 h. The cells were harvested, and reporter gene assays were carried out using the Dual-Luciferase kit (Promega). Luciferase activity was normalized to *Renilla* activity.

Gene Expression Analysis—Total RNA was isolated from cells or tissues using TRIzol reagents (Invitrogen). The RNA was reverse-transcribed using an ABI reverse transcipton kit. Quantitative PCR reactions were performed with SYBR green fluorescent dye using an ABI9300 PCR machine. Relative mRNA expression was determined by the $\Delta\Delta - C_t$ method normalized to TATA-binding protein levels. The sequences of primers used in this study are found in Table 1.

Animals—All animal experiments were performed according to procedures approved by Ulsan National Institute of Science and Technology's Institutional Animal Care and Use Committee. 5-Week-old male C57BL/6J mice were fed a high fat diet (60% kcal fat, D12492, Research Diets, Inc.). For glucose tolerant tests, mice were intraperitoneally (i.p.) injected daily 30 mg/kg of UHC1 or vehicle for 7 days and fasted overnight prior to intraperitoneal injection of 2 g/kg D-glucose. Serum insulin (Crystal Chemicals) and serum cholesterol, FFAs, triglycerides, and adiponectin were determined by ELISA (Cayman Chemicals and Millipore). For analysis of inflammatory gene expression, mice were intraperitoneally injected daily 20 mg/kg of UHC1, SR1664, or vehicle for 21 days, and adipose tissues were analyzed.

Phamacokinetic Studies—Six-week-old male Sprague-Dawley rats (220 g) were purchased from Orient Bio (Orient Bio., Inc., Seoul, Korea). The rats were housed in an air-conditioned room at temperature of 22 ± 2 °C and a relative humidity of 50 ± 10% with a 12-h dark/light cycle and allowed food and water spontaneously. Rats were fasted for 12 h before the experiment with water freely available. After an intravenous administration of SR1664 or UHCl at a dose of 1 mg/kg, blood samples were harvested into 1.5-ml Eppendorf tubes with 3.8% sodium citrate from each rat via the jugular vein before dosing and at 0.083, 0.25, 0.50, 1.0, 2.0, 3.0, 4.0, 6.0, and 24 h. After centrifugation at 3000 rpm/min for 10 min, plasma samples were transferred to neat tubes and stored at −20 °C until analysis. All pharmacokinetic parameters were evaluated by noncompartmental analysis using Phoenix WinNonlin software (version 6.0, Pharsight Co., Ltd., Mountainview, CA).

Sample Preparation—Sample preparation was performed by protein precipitation with acetonitrile. An 80-μl aliquot of acetonitrile containing internal standard was added to 20-s aliquots of serum samples and vortexed. After centrifugation (9000 × *g*, 10 min, 4 °C), a 1:1 aliquot of the supernatant was injected into the LC-MS/MS system. All prepared samples were kept in an autosampler at 4 °C until injection.

LC-MS/MS Analysis—The concentrations of SR1664 and UHC1 were measured by LC-MS/MS. The system consisted of an Triple Quad 5500 LC-MS/MS system (Applied Biosystems, Foster City, CA) equipped with an electrospray ionization interface used to generate positive ions $[M - H]^+$. The compounds were separated on a reversed-phase column (Kinetex C18, 2.1 × 100 mm, 1.7 μm particle size; Phenomenex) with an isocratic mobile phase consisting of water and acetonitrile containing 0.1% formic acid. The mobile phase was eluted using an Agilent 1290 infinity series pump (Agilent, Wilmington, DE) at 0.4 ml/min. The optimized ion spray voltage and temperature were set at 5500 V and 500 °C, respectively. The operating conditions were optimized by flow injection of an analyte and were determined as follows: CUR (curtain gas), 25 psi; GS1 (nebulizing gas), 50 psi; GS2 (turbo gas), 50 psi; collision gas (CAD), 5 psi; declustering potential (DP), 1 V; entrance potential (EP), 10

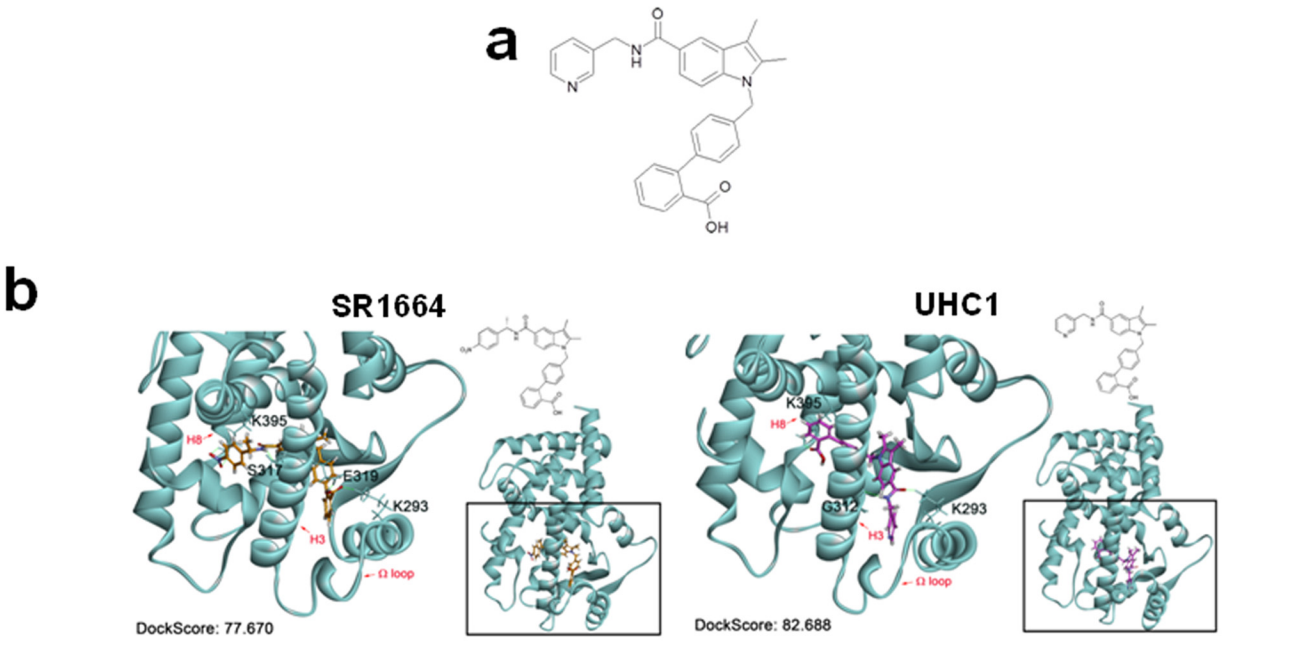

c

Descriptors	SR1664	UHC1
Molecular_weight	547.609200	489.572600
No_Rotatable_bonds	6	6
No_H_bond_acceptors	6	5
No_H_bond_donors	1	1
Topological_PSA (Å)	119.980000	87.050000
Pure water solubility (mg/L)	0.00226454	0.288063
AlogP98_value	6.730900	5.308400

d

parameters	SR1664	UHC1
Vd (ml/kg)	23043	4497
Ka (1/h)	0.16	0.56
AUC (h*ng/ml)	275.7	432.1

FIGURE 1. **Identification of UHC1 as a novel PPARγ ligand.** *a*, chemical structure of UHC1. *b*, binding mode of UHC1 or SR1664 to PPARγ LBD. Docking simulation was performed with crystal structure of PPARγ LBD (Protein Data Bank code 2HFP) and Discovery Studio® (version 1.7, Accelrys). Hydrogen bonding was illustrated by the *light-green dashed line*. *c*, chemical properties of UHC1 and SR1664. Molecular descriptors of both compounds were calculated using PreADMET software (version 2.0). *d*, pharmakokinetic parameters after intravenous administration of SR1664 and UHC1. All pharmacokinetic parameters were evaluated by noncompartmental analysis using Phoenix WinNonlin software (version 6.0). *AUC*, area under the curve.

V; collision cell exit potential (CXP), 30 V; collision gas (nitrogen) pressure, 1.8×10^{-5} Torr. Quadrupoles Q1 and Q3 were set on unit resolution. Multiple reaction-monitoring mode using specific precursor/product ion transition was used for the quantification. The ions were detected by monitoring the transitions of m/z 548.106 → 382.1 for SR1664 (collision energy, 21 eV) and 490.03 → 211.0 for UHC1 (collision energy, 45 eV). The analytical data were processed by Analyst software (version 1.5.1; Applied Biosystems, Foster City, CA).

RESULTS

Identification of the Novel PPARγ Ligand UHC1—We demonstrated previously that CDK5 can phosphorylate PPARγ and PPARγ ligands that can block PPARγ phosphorylation exhibit improved insulin sensitivity (13, 14). To identify novel anti-diabetic drugs, we performed *in silico* docking studies for rational drug design. Of particular interest was SR1664, which has non-agonism of PPARγ. Although SR1664 has potent anti-diabetic activity *in vivo*, it has poor pharmacokinetics and solubility. Therefore, we performed a modular synthetic approach to prepare a series of SR1664 analogs. We then tested the *in vitro* binding affinity of these compounds for the PPARγ LBD and assessed the transcriptional activation of PPARγ. One of these analogs, UHC1, was identified as a promising candidate (Fig. 1*a*).

Next, we compared the *in silico* docking simulations of UHC1 and SR1664 (Fig. 1*b*). The docking score of UHC1 for the LBD of PPARγ revealed that UHC1 might fit better than SR1664 in the proper binding mode. Interestingly, a carboxylic acid moiety of UHC1 was assumed to interact with Lys-395 in helix 8 of the PPARγ LBD, whereas the opposite mode of binding was predicted in the case of SR1664. Although UHC1 and SR1664 have different modes of binding, their intermolecular interactions between the ligand and PPARγ were similar; helix 3, helix 8, and the loop were affected by ligand binding (Fig. 1*b*). We next calculated the molecular descriptors, from which we can predict the physicochemical properties of UHC1 and SR1664 by comparing the topological polar surface area (UHC1, 87 $Å^2$; SR1664, 120 $Å^2$). In pharmacokinetic analysis,

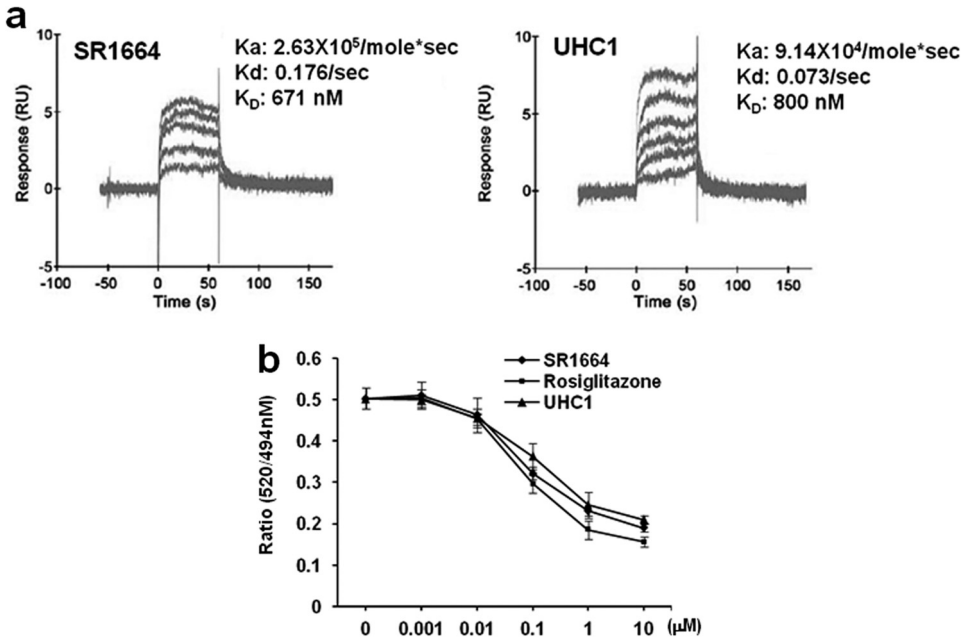

FIGURE 2. **Binding affinity of UHC1 or SR1664 to PPARγ LBD.** *a*, sensorgram of surface plasmon resonance (*SPR*) assay was obtained with a Biacore T100 instrument (GE Healthcare). Data were analyzed using the Biacore T100 Evaluation software (GE Healthcare). The dissociation constant (K_D) was calculated by fitting the sensorgrams to the 1:1 binding model of each ligand (UHC1 or SR1664) with hPPARγ LBD. *b*, the binding affinity of rosiglitazone, UHC1, or SR1664 to PPARγ by LanthaScreen assay. *Error bars* are S.E. ($n = 3$). *RU*, response units.

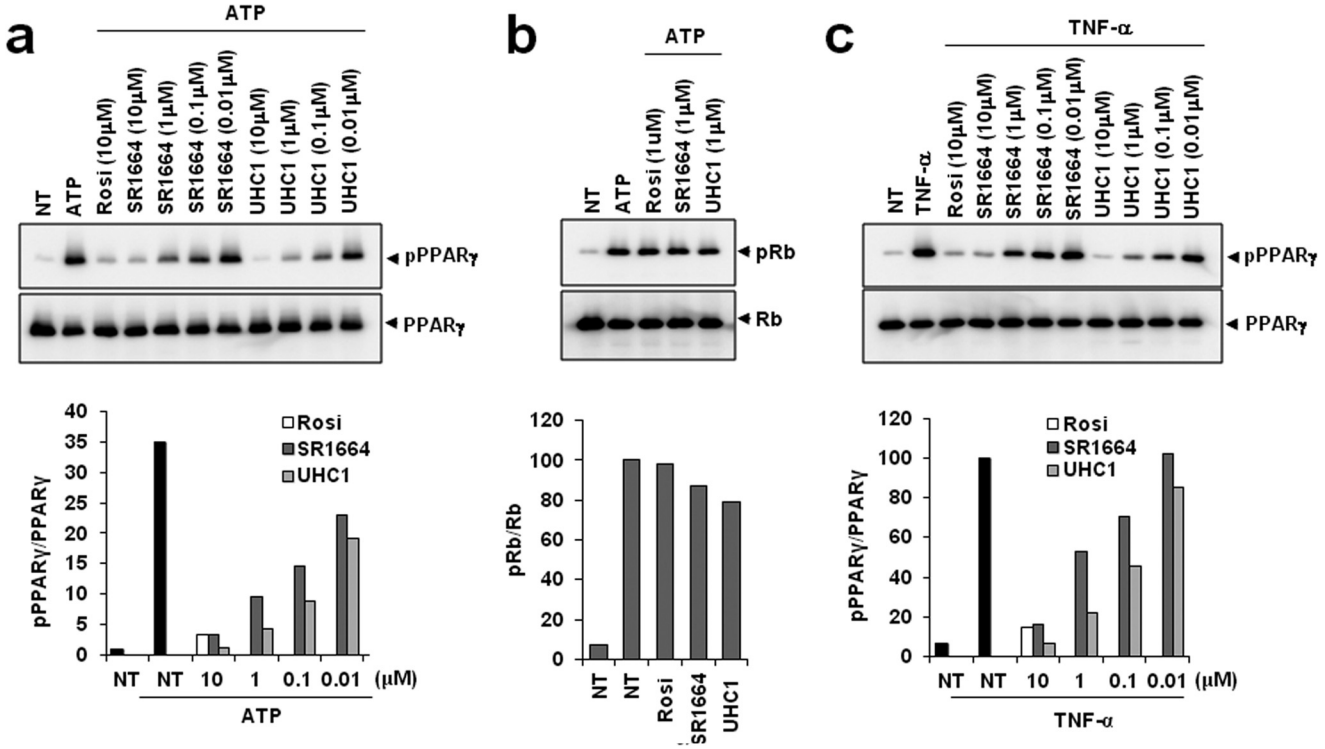

FIGURE 3. **Inhibition of CDK5-mediated PPARγ phosphorylation by UHC1.** *a*, *in vitro* CDK5 assay on full-length PPARγ incubated with rosiglitazone, UHC1, or SR1664. *b*, phosphorylation of Rb after treating with rosiglitazone (*Rosi*), UHC1, or SR1664. *c*, TNF-α-induced phosphorylation of PPARγ in adipocytes expressing PPARγ treated with rosiglitazone, UHC1, or SR1664. *NT*, not treated.

UHC1 showed lower tissue distribution (V_d) and higher elimination rate constant (K_a) than those of SR1664, suggesting the solubility of UHC1 is significantly improved (15) (Fig. 1, *c* and *d*). Furthermore, we assessed the direct binding affinity of UHC1 and SR1664 to the PPARγ LBD using surface plasmon resonance (Fig. 2*a*). Both SR1664 and UHC1 had strong binding affinity for the PPARγ LBD, and the effects were dose-dependent. These results suggest that UHC1 interacts with the PPARγ LBD and that it has more favorable chemical properties than SR1664. Based on a LanthaScreen TR-FRET competitive binding assay (Fig. 2*b*) and surface plasmon resonance analyses (Fig. 2*a*), UHC1 had a half-maximum inhibitory concentration

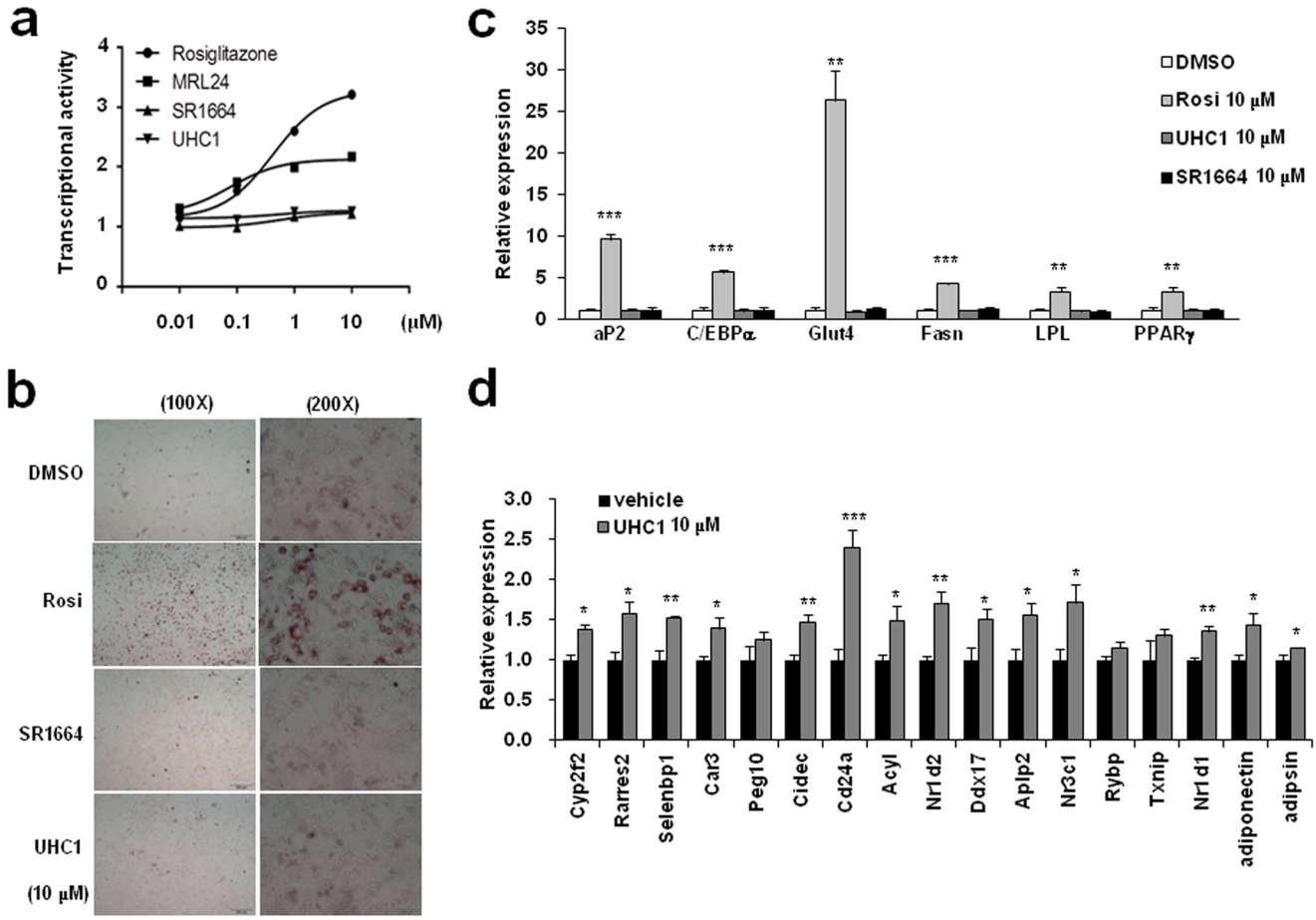

FIGURE 4. **Non-agonism of UHC1.** *a*, transcriptional activity of a PPAR-derived reporter gene in HEK-293 cells following treatment with rosiglitazone (*Rosi*; 10 μmol/liter), UHC1 (10 μmol/liter), or SR1664 (10 μmol/liter). *b*, lipid accumulation in differentiated 3T3-L1 adipocytes following Oil-red O staining. Expression of adipocyte-enriched genes (*c*) and gene set regulated by PPARγ phosphorylation (*d*) in these cells was analyzed by qPCR. *Error bars* are S.E. ($n = 3$). *, $p < 0.05$; **, $p < 0.01$; ***, $p < 0.001$ compared with control. *DMSO*, dimethyl sulfoxide.

(IC_{50}) for the PPARγ LBD of ~800 nmol/l to PPARγ LBD, which is 6–7-fold higher than that of rosiglitazone, but much lower than that of pioglitazone (16).

UHC1 Specifically Blocks CDK5-mediated PPARγ Phosphorylation—Next, we assessed whether UHC1 modulated CDK5-mediated PPARγ phosphorylation using *in vitro* kinase assays. As shown in Fig. 3*a*, UHC1 specifically inhibited PPARγ phosphorylation in a dose-dependent manner. Interestingly, UHC1 caused more potent inhibition of PPARγ phosphorylation than SR1664. Although the binding affinity of UHC1 for PPARγ was slightly weaker than that of rosiglitazone (Fig. 2*b*), UHC1 had a more potent effect on inhibiting CDK5-mediated PPARγ phosphorylation at a 10 μmol/liter concentration than rosiglitazone (Fig. 3*a*). UHC1 also inhibited TNF-α-mediated PPARγ phosphorylation in adipocytes (Fig. 3*c*). Importantly, UHC1 did not block CDK5-mediated Rb phosphorylation, suggesting that UHC1 affects PPARγ selectively and directly (Fig. 3*b*). Taken together, these data suggest that UHC1 is a novel PPARγ ligand with strong affinity for PPARγ and that it blocks specifically CDK5-mediated PPARγ phosphorylation.

UHC1 Does Not Affect Adipogenesis—It has been well known that PPARγ activation is necessary and sufficient for adipocytes differentiation (4). Therefore, if UHC1 is a classical transcriptional agonist, it would stimulate the differentiation of preadipocytes into mature adipocytes (17). As shown in Fig. 4*a*, treatment with UHC1 did not stimulate PPARγ transcriptional activity, as assessed by a luciferase assay in HEK-293 cells expressing a PPRE-containing luciferase construct. Consistent with a previous study (14), MRL24 was a partial agonist of PPARγ, whereas SR1664 did not have any agonism of PPARγ (Fig. 4*a*). In addition, rosiglitazone potently stimulated adipocytes differentiation, whereas UHC1or SR1664 did not increase lipid accumulation at the same dose of ligands (10 μmol/liter) (Fig. 4*b*). Moreover, the expression of classical adipogenic markers was increased significantly by rosiglitazone, but not by UHC1 or SR1664 (Fig. 4*c*). Furthermore, UHC1 significantly regulated the expression of 14/17 genes, which were dystregulated by CDK5-mediated PPARγ phosphorylation in fully differentiated adipocytes (Fig. 4*d*) (13). Therefore, these data suggest that UHC1 is not a classical transcriptional agonist of PPARγ and specifically regulates CDK5-mediated PPARγ phosphorylation.

UHC1 Has Anti-inflammatory Effects on 3T3-L1 Adipocytes and Macrophages—It has been suggested that the activation of PPARγ by TZDs ameliorates inflammation in many different tissues by inhibiting the expression of proinflammatory genes and/or activating anti-inflammatory genes (18–20). In adipose tissue, adipocytes and infiltrated macrophages are important

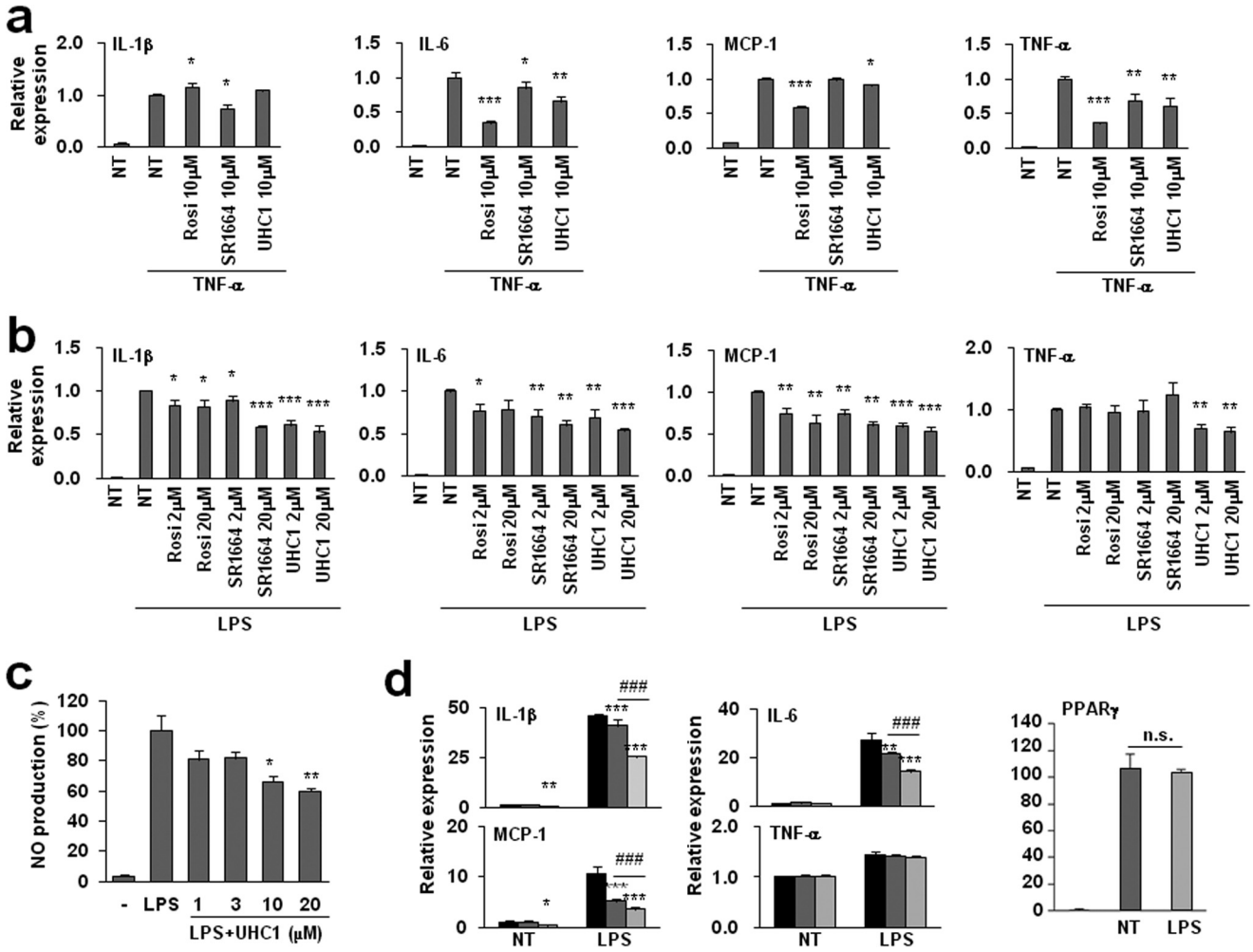

FIGURE 5. **Suppression of proinflammatory gene expression by UHC1 *in vitro*.** *a*, differentiated 3T3-L1 adipocytes were incubated with rosiglitazone (*Rosi*), UHC1, or SR1664 for 24 h and were treated with TNF-α (10 ng/ml) for 3 h. *b*, Raw264.7 macrophages were incubated with rosiglitazone, UHC1, or SR1664 at specific concentration for 24 h and were treated with LPS (100 ng/ml) for 6 h. Relative gene expression was determined by qPCR. *c*, Raw264.7 cells were preincubated with UHC1 at specific concentration for 1 h and were treated with LPS (100 ng/ml) for 24 h. The amount of nitrite in cell-free culture supernatants was measured using Griess reagent. *d*, Raw264.7 macrophages expressing PPARγWT or PPARγS273A were treated with LPS (100 ng/ml) for 6 h. Relative gene expression was determined by qPCR. *Error bars* are S.E. ($n = 3$). *, $p < 0.05$; **, $p < 0.01$; ***, $p < 0.001$ compared with control; ###, $p < 0.001$ compared between PPARγWT and PPARγS273A. *n.s.*, not significant; *NT*, not treated.

sources of inflammatory molecules; therefore, we assessed whether UHC1 suppressed the inflammatory response in adipocytes and macrophages. Treating 3T3-L1 adipocytes with TNF-α stimulated the expression of proinflammatory genes, including interleukin-1β (IL-1β), IL-6, monocyte chemoattractant protein-1 (MCP-1), and TNF-α (Fig. 5*a*). Pre-incubation with UHC1 suppressed the TNF-α-induced proinflammatory response (Fig. 5*a*). Similar results were obtained in Raw264.7 macrophages following treatment with lipopolysaccharide (LPS) (Fig. 5*b*). In addition, UHC1 reduced LPS-induced nitric oxide (NO) production, which is critical for the inflammatory response in Raw264.7 macrophages (Fig. 5*c*) (21). Importantly, the inhibitory effects of UHC1 on proinflammatory gene expression were stronger than SR1664 at the same concentration (Fig. 5, *a* and *b*).

To determine whether the phosphorylation of PPARγ at Ser-273 played a role in the proinflammatory response, we measured LPS-induced inflammation after overexpressing wild type PPARγ (PPARγWT) or a phosphorylation-deficient PPARγ mutant (PPARγS273A) in Raw264.7 macrophages. Surprisingly, PPARγS273A suppressed LPS-induced IL-1β, MCP-1, and IL-6 expression more efficiently than PPARγWT without altering the expression of PPARγ itself. However, PPARγS273A did not suppress the expression of TNF-α, whereas treatment with UHC1 did, suggesting that the phosphorylation of PPARγ at Ser-273 regulates the inflammatory response, and UHC1 might regulate specific proinflammatory genes in a PPARγ-dependent and -independent manner.

UHC1 Has Potent Anti-diabetic Effects in Vivo—To explore the effect of UHC1 *in vivo*, we treated HFD-fed mice with UHC1 or SR1664. As shown in Fig. 6*a*, treatment with 30 mg/kg/day UHC1 or SR1664 for 7 days reduced PPARγ phosphorylation at Ser-273 in adipose tissue. Importantly, treatment with UHC1 dramatically improved the glucose tolerance of HFD-fed mice and reduced their fasting glucose and insulin levels and percent of HbA1c without changing their body weight (Fig. 6, *b*–*e* and *j*). Although SR1664 also improved glucose tolerance, UHC1 exerted more potent effects on glucose

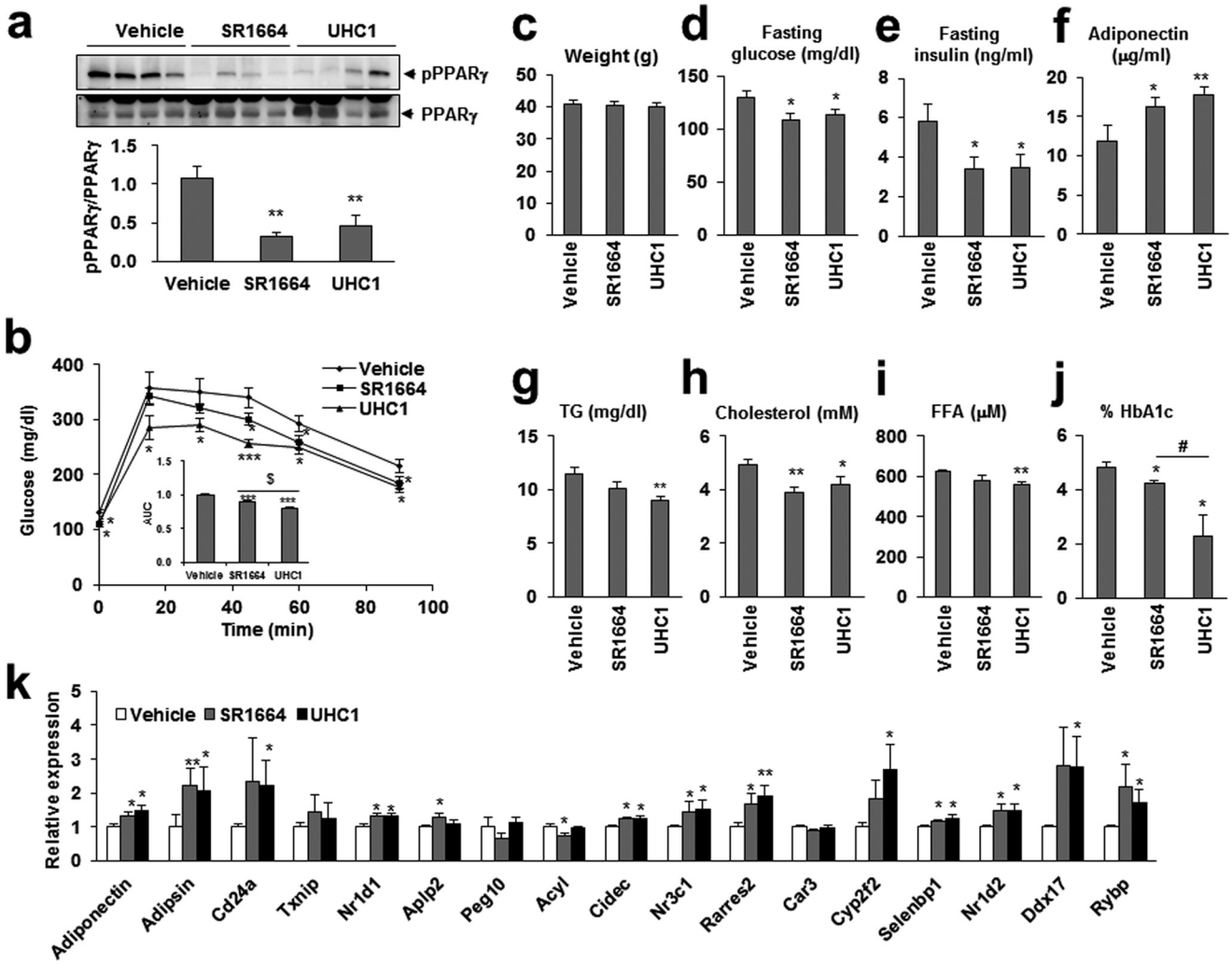

FIGURE 6. **Anti-diabetic action of UHC1 *in vivo*.** *a*, phosphorylation of PPARγ in white adipose tissue. Quantification of PPARγ phosphorylation compared with total PPARγ was performed. *b*, glucose tolerant test in HFD-fed mice treated with vehicle, SR1664, or UHC1 (30 mg/kg). Fasting body weight (*c*), fasting glucose (*d*), fasting insulin (*e*), serum adiponectin (*f*), fasting triglyceride (*TG*) (*g*), fasting cholesterol (*h*), and fasting FFA (*i*) were determined after HFD-fed mice treated with vehicle, UHC1, or SR1664. *j*, percent of HbA1c were determined after *ob*/*ob* mice treated with vehicle, UHC1 (20 mg/kg), or SR1664 (20 mg/kg) for 21 days. *k*, expression of gene set regulated by PPARγ phosphorylation in white adipose tissue. *Error bars* are S.E. ($n = 7$). *, $p < 0.05$; **, $p < 0.01$; ***, $p < 0.001$ compared with vehicle; $, $p < 0.001$; #, $p < 0.05$ compared with SR1664. *AUC*, area under the curve.

tolerance (Fig. 6*b*). In addition, reductions in serum basal triglycerides, cholesterol, and FFAs were detected, suggesting improved insulin sensitivity in the adipose tissue of UHC1-treated mice (Fig. 6, *g*–*i*). Furthermore, UHC1 altered the expression of 12 of the 17 genes that were dysregulated by CDK5-mediated PPARγ phosphorylation (Fig. 6*k*) (13). For example, the mRNA and serum levels of adiponectin, which is known to protect against obesity and diabetes, were increased by UHC1 (Fig. 6, *f* and *k*) (22). These data suggest that the anti-diabetic PPARγ ligand UHC1 inhibited CDK5-mediated PPARγ phosphorylation *in vivo* and reversed the changes in gene expression associated with PPARγ phosphorylation.

UHC1 Ameliorates Inflammation in Vivo—To further investigate the effect of UHC1 on adipose tissue, we assessed the expression of genes related to inflammation and lipolysis. As shown in Fig. 7, *a* and *b*, treatment with UHC1 for 7 days in high-fat fed mice reduced significantly IL-6 (a proinflammatory M1 macrophage marker), whereas IL-10 and arginase (anti-inflammatory M2 macrophage markers) were increased. Furthermore, when we administrated with UHC1 or SR1664 for 21 days in high fat-fed mice, the expressions of proinflammatory genes including IL-1β, IL-6, MCP-1, and TNF-α were reduced significantly, and these effects were more dramatic with UHC1 treatment than SR1664 (Fig. 7*c*). Taken together, these results strongly suggest that UHC1 has more potent anti-inflammatory activity than SR1664.

It has shown that the products of lipolysis such as fatty acids induce inflammation in adipose tissue (23, 24). Therefore, we next analyzed the expression of genes that are associated with lipolysis. As shown in Fig. 7*d*, HFD-fed mice treated with UHC1 exhibited dramatically reduced expression of monoacylglycerol lipase (MGL) and hormone-sensitive lipase (HSL), which play roles in lipolysis and energy metabolism (25, 26). Consistent with the observations described above, UHC1 exerted these effects more potently than SR1664. Decreased expression of lipolysis-related genes was well correlated with reduced circulating FFA levels in the UHC1-treated mice (Fig. 6*i*). Together, these data suggest that UHC1 effectively suppressed the inflam-

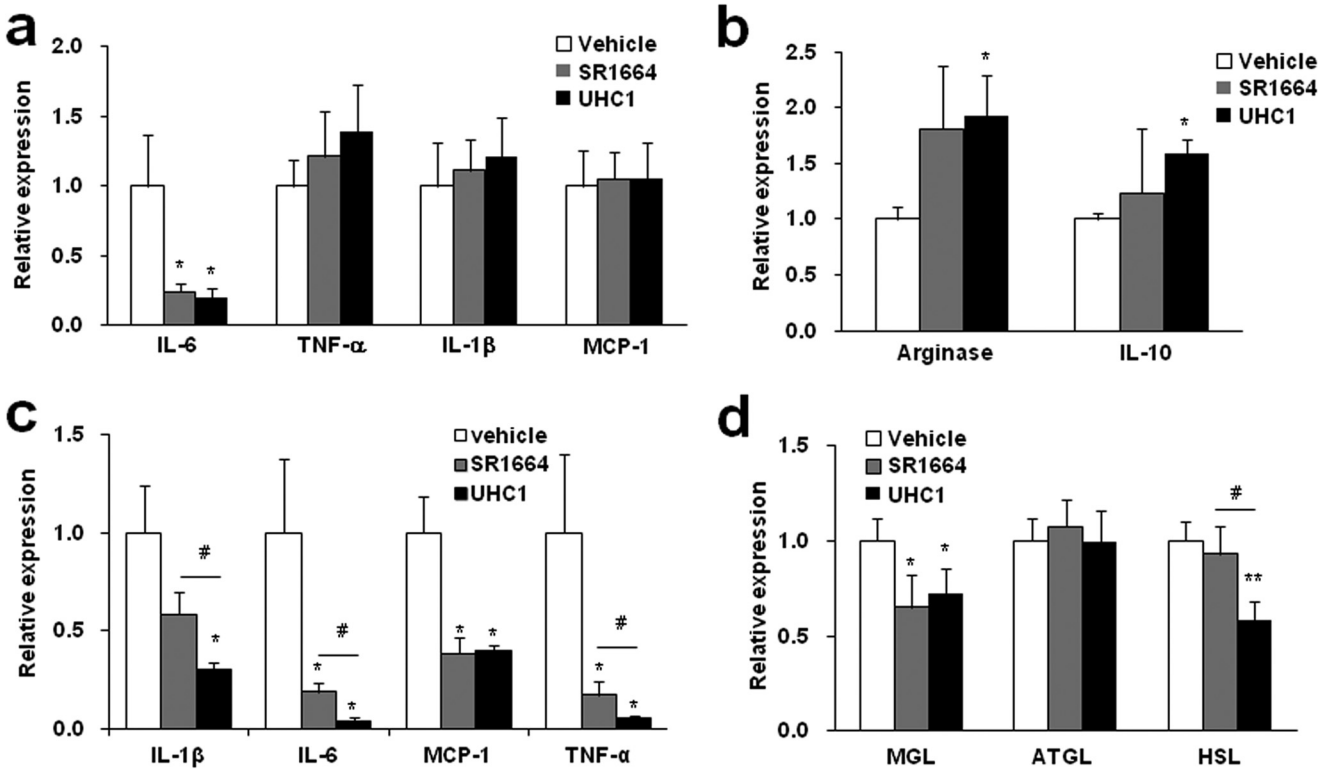

FIGURE 7. **Anti-inflammatory action of UHC1 *in vivo*.** M1 macrophage-specific marker genes (*a*), M2 macrophage-specific marker genes (*b*), lipolysis involved genes (*d*) were analyzed by qPCR followed by 7-day treatment with SR1664 (30 mg/kg) or UHC1 (30 mg/kg). *c*, M1 macrophage-specific marker genes were analyzed by qPCR followed by 21-day treatment with SR1664 (20 mg/kg) or UHC1 (20 mg/kg). *Error bars* are S.E. ($n = 7$). *, $p < 0.05$; **, $p < 0.01$ compared with vehicle; #, $p < 0.05$ compared with SR1664. *ATGL*, adipose triglyceride lipase.

matory response by regulating the expression of proinflammatory and anti-inflammatory genes. These effects might be associated with reduced levels of FFAs from lipolysis and could eventually improve insulin sensitivity.

UHC1 Exerts Its Pharmacological Properties without Side Effects—TZDs such as rosiglitazone cause weight gain, fluid retention, and bond fractures, which all contribute to increased cardiac dysfunction (27, 28). These severe side effects are thought to be due to off-target actions by TZDs. Therefore, we hypothesized that UHC1, which is not a classical agonist of PPARγ, might avoid these side effects. As shown in Fig. 8, HFD-fed mice treated with rosiglitazone for 14 days exhibited increased body weight and a significant reduced hematocrit. However, UHC1 had no effect on body weight or hemodilution (Fig. 8, *a* and *b*), whereas both rosiglitazone and UHC1 improved glucose tolerance at similar level (Fig. 8*c*). These data suggest that UHC1 exerts potent anti-diabetic actions without causing the same side effects as TZDs *in vivo*.

DISCUSSION

TZDs have been widely used to treat type 2 diabetes (1, 2, 6). However, Avandia (rosiglitazone) was withdrawn in 2010 due to severe side effects such as heart failure, weight gain, and fluid retention. Recently, we reported that the non-agonist PPARγ ligand SR1664 blocked CDK5-mediated PPARγ phosphorylation and exerted potent anti-diabetic effects with no side effects (14). However, SR1664 has poor pharmacokinetics and solubility. Therefore, we improved the chemical properties of SR1664 using *in silico* docking studies for rational drug design. In the current study, we demonstrated that the novel PPARγ ligand UHC1 has more potent anti-diabetic activity than SR1664 *in vivo* (Fig. 6). Furthermore, UHC1 has dramatically improved chemical properties (Fig. 1, *b–d*) and more potently inhibited CDK5-mediated phosphorylation of PPARγ and the proinflammatory response compared with SR1664, both *in vitro* and *in vivo* (Figs. 3, 5, and 7). These data indicate that UHC1 could be a novel therapeutic agent to target PPARγ by overcoming the disadvantages of SR1664.

Chronic inflammation is associated with obesity, insulin resistance, and type-2 diabetes (29, 30). Therefore, we hypothesized that UHC1 regulates the inflammatory response. As expected, treatment with UHC1 significantly inhibited TNF-α- or LPS-induced proinflammatory responses in adipocytes and macrophages, respectively (Fig. 5). In adipose tissues, UHC1 also reduced IL-1β, IL-6, MCP-1, and TNF-α expression, consistent with *in vitro* experiments. Adipose tissue macrophages are classified with classically activated M1 macrophages and alternatively activated M2 macrophages (30, 31). The M1 macrophages contribute to the development of insulin resistance, whereas alternatively activated the M2 macrophages ameliorate insulin resistance (30). In our study, UHC1 concomitantly increased the M2 macrophage marker genes arginase and IL-10 (Fig. 7*b*). Thus, these results suggest that UHC1 can redirect adipose tissue macrophages from the M1 to the M2 polarization state, which contributes to the anti-inflammatory responses of adipose tissue macrophages in HFD-fed mice. Consistent with this, previous reports demonstrated that the

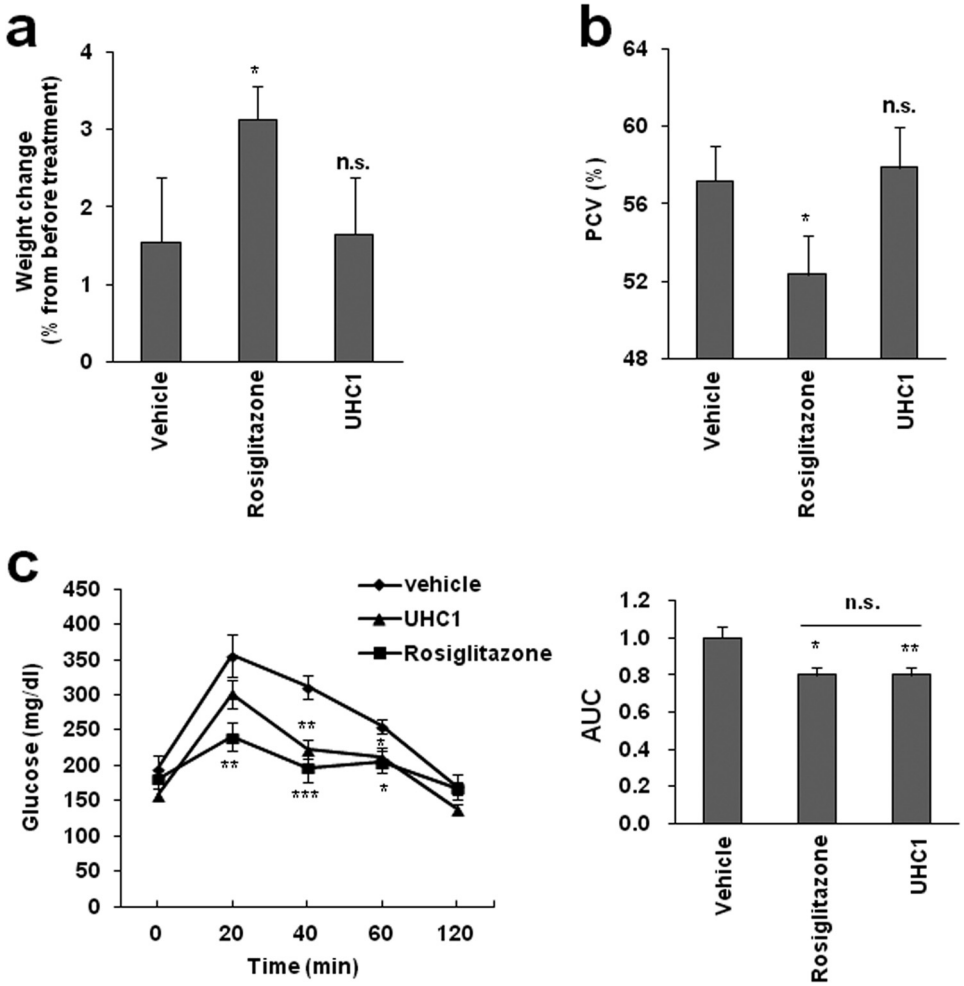

FIGURE 8. **The effect of UHC1 on weight gain or fluid retention.** *a*, whole-body weight changes in HFD-fed mice treated with rosiglitazone (10 mg/kg) or UHC1 (30 mg/kg) for 14 days. *b*, packed cell volume (*PCV*) in whole blood from these mice. *Error bars* are S.E. ($n = 6$). *c*, glucose tolerant test in HFD-fed mice treated with vehicle, rosiglitazone (10 mg/kg), or UHC1 (30 mg/kg) for 7 days. *Error bars* are S.E. *, $p < 0.05$; **, $p < 0.01$; ***, $p < 0.001$ compared with vehicle. *n.s.*, not significant. *AUC*, area under the curve.

activation of PPARγ by pioglitazone promoted recruitment and alternatively activation of adipose tissue macrophages, reduced inflammation, and improved insulin sensitivity (32–35). We also revealed that blocking the phosphorylation of PPARγ at Ser-273 could suppress LPS-mediated proinflammatory gene expression (Fig. 5*d*). Therefore, it is likely that modulating PPARγ phosphorylation is an important mechanism for the anti-diabetic effects of PPARγ ligands in macrophages.

The lipolysis of adipose tissue leads to the hydrolysis of triglycerides and the release of FFAs (36). Circulating levels of FFAs are usually elevated in obesity and type 2 diabetes (37), where they activate the classical inflammatory response in macrophages; this can lead to the development of insulin resistance and metabolic syndrome. Therefore, adipose tissue lipolysis is a major target for anti-diabetes drug development (37, 38). Adipose triglyceride lipase is the rate-limiting enzyme for lipolysis, and mice lacking this enzyme exhibit reduced levels of plasma FFAs (39, 40). Although the expression of adipose triglyceride lipase was unchanged by the UHC1 treatment in our study, UHC1 reduced the expression of MGL and HSL (Fig. 7*d*). MGL is a key enzyme in lipolysis that converts monoglycerol to glycerol and FFAs. HSL can hydrolyze triacylglycerols to release FFAs. The physiological role of MGL was revealed in MGL-deficient mice, which exhibited impaired lipolysis and improved diet-induced insulin resistance (26). In addition, the impaired lipolysis by disrupting HSL expression affected HFD-induced obesity and adipose-derived hormone levels (25). The UHC1-mediated decrease in MGL or HSL gene expression is consistent with the reduced circulating FFA levels in UHC1-treated HFD-fed mice (Fig. 6*i*). Together, our results suggest that blocking phosphorylation of PPARγ with UHC1 efficiently reduced the inflammatory response *in vitro* and *in vivo*, and these anti-inflammatory effects were partially due to reducing the release of FFAs from adipose tissue.

Severe side effects of TZDs, including weight gain and fluid retention, occur rapidly in both humans and mice (12, 27, 28). As shown in Fig. 8, increased body weight and fluid retention were observed in mice treated with rosiglitazone for 2 weeks. However, UHC1 did not cause these effects but dramatically improved insulin sensitivity. Although long term administration must be performed to evaluate whether UHC1 exerts any other side effects, these data suggest that UHC1 improves insu-

lin sensitivity without stimulating acute fluid retention or weight gain.

Acknowledgments—We thank Dr. Bruce M. Spiegelman for supporting phospho-specific antibody against Ser-273 residue. We thank Dr. Eung Kyun Kim at UNIST OLYMPUS Biomed Imaging Center (UOBC) for supporting microscopic images. The pharmacokinetic study was supported by the Laboratory Animal Center in Daegu-Gyeongbuk Medical Innovation Foundation.

REFERENCES

1. Evans, R. M., Barish, G. D., and Wang, Y. X. (2004) PPARs and the complex journey to obesity. *Nat. Med.* **10,** 355–361
2. Tontonoz, P., and Spiegelman, B. M. (2008) Fat and beyond: the diverse biology of PPARγ. *Ann. Rev. Biochem.* **77,** 289–312
3. Willson, T. M., Lambert, M. H., and Kliewer, S. A. (2001) Peroxisome proliferator-activated receptor γ and metabolic disease. *Ann. Rev. Biochem.* **70,** 341–367
4. Tontonoz, P., Hu, E., Graves, R. A., Budavari, A. I., and Spiegelman, B. M. (1994) mPPAR γ 2: tissue-specific regulator of an adipocyte enhancer. *Genes Dev.* **8,** 1224–1234
5. Forman, B. M., Tontonoz, P., Chen, J., Brun, R. P., Spiegelman, B. M., and Evans, R. M. (1995) 15-Deoxy-δ 12, 14-prostaglandin J2 is a ligand for the adipocyte determination factor PPAR γ. *Cell* **83,** 803–812
6. Lehmann, J. M., Moore, L. B., Smith-Oliver, T. A., Wilkison, W. O., Willson, T. M., and Kliewer, S. A. (1995) An antidiabetic thiazolidinedione is a high affinity ligand for peroxisome proliferator-activated receptor γ (PPAR γ). *J. Biol. Chem.* **270,** 12953–12956
7. Moras, D., and Gronemeyer, H. (1998) The nuclear receptor ligand-binding domain: structure and function. *Curr. Opin. Cell Biol.* **10,** 384–391
8. Chandra, V., Huang, P., Hamuro, Y., Raghuram, S., Wang, Y., Burris, T. P., and Rastinejad, F. (2008) Structure of the intact PPAR-γ-RXR- nuclear receptor complex on DNA. *Nature* **456,** 350–356
9. Higgins, L. S., and Depaoli, A. M. (2010) Selective peroxisome proliferator-activated receptor γ (PPARγ) modulation as a strategy for safer therapeutic PPARγ activation. *Amer. J. Clin. Nutr.* **91,** 267S–272S
10. Bruning, J. B., Chalmers, M. J., Prasad, S., Busby, S. A., Kamenecka, T. M., He, Y., Nettles, K. W., and Griffin, P. R. (2007) Partial agonists activate PPARγ using a helix 12 independent mechanism. *Structure* **15,** 1258–1271
11. Elbrecht, A., Chen, Y., Adams, A., Berger, J., Griffin, P., Klatt, T., Zhang, B., Menke, J., Zhou, G., Smith, R. G., and Moller, D. E. (1999) L-764406 is a partial agonist of human peroxisome proliferator-activated receptor γ: the role of Cys^{313} in ligand binding. *J. Biol. Chem.* **274,** 7913–7922
12. Zhang, F., Lavan, B. E., and Gregoire, F. M. (2007) Selective modulators of PPAR-γ activity: molecular aspects related to obesity and side-effects. *PPAR. Res.* **2007,** 32696
13. Choi, J. H., Banks, A. S., Estall, J. L., Kajimura, S., Boström, P., Laznik, D., Ruas, J. L., Chalmers, M. J., Kamenecka, T. M., Blüher, M., Griffin, P. R., and Spiegelman, B. M. (2010) Anti-diabetic drugs inhibit obesity-linked phosphorylation of PPARγ by Cdk5. *Nature* **466,** 451–456
14. Choi, J. H., Banks, A. S., Kamenecka, T. M., Busby, S. A., Chalmers, M. J., Kumar, N., Kuruvilla, D. S., Shin, Y., He, Y., Bruning, J. B., Marciano, D. P., Cameron, M. D., Laznik, D., Jurczak, M. J., Schürer, S. C., Vidović, D., Shulman, G. I., Spiegelman, B. M., and Griffin, P. R. (2011) Antidiabetic actions of a non-agonist PPARγ ligand blocking Cdk5-mediated phosphorylation. *Nature* **477,** 477–481
15. Henchoz Y, Bard B, Guillarme D, Carrupt P. A., Veuthey J. L., and Martel S. (2009) Analytical tools for the physicochemical profiling of drug candidates to predict absorption/distribution. *Anal Bioanal. Chem.* **394,** 707–729
16. Young, P. W., Buckle, D. R., Cantello, B. C., Chapman, H., Clapham, J. C., Coyle, P. J., Haigh, D., Hindley, R. M., Holder, J. C., Kallender, H., Latter, A. J., Lawrie, K. W., Mossakowska, D., Murphy, G. J., Roxbee Cox, L., and Smith, S. A. (1998) Identification of high-affinity binding sites for the insulin sensitizer rosiglitazone (BRL-49653) in rodent and human adipocytes using a radioiodinated ligand for peroxisomal proliferator-activated receptor γ. *J. Pharmacol. Exp. Ther.* **284,** 751–759
17. Tontonoz, P., Hu, E., and Spiegelman, B. M. (1994) Stimulation of adipogenesis in fibroblasts by PPAR γ 2, a lipid-activated transcription factor. *Cell* **79,** 1147–1156
18. Jiang, C., Ting, A. T., and Seed, B. (1998) PPAR-γ agonists inhibit production of monocyte inflammatory cytokines. *Nature* **391,** 82–86
19. Ricote, M., Li, A. C., Willson, T. M., Kelly, C. J., and Glass, C. K. (1998) The peroxisome proliferator-activated receptor-γ is a negative regulator of macrophage activation. *Nature* **391,** 79–82
20. Welch, J. S., Ricote, M., Akiyama, T. E., Gonzalez, F. J., and Glass, C. K. (2003) PPARγ and PPARδ negatively regulate specific subsets of lipopolysaccharide and IFN-γ target genes in macrophages. *Proc. Natl. Acad. Sci. U.S.A.* **100,** 6712–6717
21. Laskin, D. L., and Pendino, K. J. (1995) Macrophages and inflammatory mediators in tissue injury. *Ann. Rev. Pharm. Toxicol.* **35,** 655–677
22. Trujillo, M. E., and Scherer, P. E. (2006) Adipose tissue-derived factors: impact on health and disease. *Endocr. Rev.* **27,** 762–778
23. Wang, L., Gill, R., Pedersen, T. L., Higgins, L. J., Newman, J. W., and Rutledge, J. C. (2009) Triglyceride-rich lipoprotein lipolysis releases neutral and oxidized FFAs that induce endothelial cell inflammation. *J. Lipid Res.* **50,** 204–213
24. Horrillo, R., González-Périz, A., Martínez-Clemente, M., López-Parra, M., Ferré, N., Titos, E., Morán-Salvador, E., Deulofeu, R., Arroyo, V., and Clària, J. (2010) 5-Lipoxygenase activating protein signals adipose tissue inflammation and lipid dysfunction in experimental obesity. *J. Immunol.* **184,** 3978–3987
25. Harada, K., Shen, W. J., Patel, S., Natu, V., Wang, J., Osuga, J., Ishibashi, S., and Kraemer, F. B. (2003) Resistance to high-fat diet-induced obesity and altered expression of adipose-specific genes in HSL-deficient mice. *Am. J. Physiol. Endocrinol. Metab.* **285,** E1182–E1195
26. Taschler, U., Radner, F. P., Heier, C., Schreiber, R., Schweiger, M., Schoiswohl, G., Preiss-Landl, K., Jaeger, D., Reiter, B., Koefeler, H. C., Wojciechowski, J., Theussl, C., Penninger, J. M., Lass, A., Haemmerle, G., Zechner, R., and Zimmermann, R. (2011) Monoglyceride lipase deficiency in mice impairs lipolysis and attenuates diet-induced insulin resistance. *J. Biol. Chem.* **286,** 17467–17477
27. Nesto, R. W., Bell, D., Bonow, R. O., Fonseca, V., Grundy, S. M., Horton, E. S., Le Winter, M., Porte, D., Semenkovich, C. F., Smith, S., Young, L. H., and Kahn, R. (2004) Thiazolidinedione use, fluid retention, and congestive heart failure: a consensus statement from the American Heart Association and American Diabetes Association. *Diabetes Care.* **27,** 256–263
28. Kahn, S. E., Zinman, B., Lachin, J. M., Haffner, S. M., Herman, W. H., Holman, R. R., Kravitz, B. G., Yu, D., Heise, M. A., Aftring, R. P., Viberti, G., and Diabetes Outcome Progression Trial (ADOPT) Study Group (2008) Rosiglitazone-associated fractures in type 2 diabetes: an analysis from a diabetes outcome progression trial (ADOPT). *Diabetes Care.* **31,** 845–851
29. Donath, M. Y., and Shoelson, S. E. (2011) Type 2 diabetes as an inflammatory disease. *Nat. Rev. Immunol.* **11,** 98–107
30. Shoelson, S. E., Lee, J., and Goldfine, A. B. (2006) Inflammation and insulin resistance. *J. Clin. Invest.* **116,** 1793–1801
31. Sica, A., and Mantovani, A. (2012) Macrophage plasticity and polarization: *in vivo* veritas. *J. Clin. Invest.* **122,** 787–795
32. Bouhlel, M. A., Derudas, B., Rigamonti, E., Dièvart, R., Brozek, J., Haulon, S., Zawadzki, C., Jude, B., Torpier, G., Marx, N., Staels, B., and Chinetti-Gbaguidi, G. (2007) PPARγ activation primes human monocytes into alternative M2 macrophages with anti-inflammatory properties. *Cell Metab.* **6,** 137–143
33. Odegaard, J. I., Ricardo-Gonzalez, R. R., Goforth, M. H., Morel, C. R., Subramanian, V., Mukundan, L., Red Eagle, A., Vats, D., Brombacher, F., Ferrante, A. W., and Chawla, A. (2007) Macrophage-specific PPARγ controls alternative activation and improves insulin resistance. *Nature* **447,** 1116–1120
34. Shaul, M. E., Bennett, G., Strissel, K. J., Greenberg, A. S., and Obin, M. S. (2010) Dynamic, M2-like remodeling phenotypes of CD11c+ adipose tissue macrophages during high-fat diet-induced obesity in mice. *Diabetes* **59,** 1171–1181
35. Stienstra, R., Duval, C., Keshtkar, S., van der Laak, J., Kersten, S., and Müller, M. (2008) Peroxisome proliferator-activated receptor γ activation promotes infiltration of alternatively activated macrophages into adipose

tissue. *J. Biol. Chem.* **283,** 22620–22627
36. Holm, C., Osterlund, T., Laurell, H., and Contreras, J. A. (2000) Molecular mechanisms regulating hormone-sensitive lipase and lipolysis. *Annu. Rev. Nutr.* **20,** 365–393
37. Unger, R. H. (2002) Lipotoxic diseases. *Ann. Rev. Med.* **53,** 319–336
38. Karpe, F., Dickmann, J. R., and Frayn, K. N. (2011) Fatty acids, obesity, and insulin resistance: time for a reevaluation. *Diabetes* **60,** 2441–2449
39. Huijsman, E., van de Par, C., Economou, C., van der Poel, C., Lynch, G. S., Schoiswohl, G., Haemmerle, G., Zechner, R., and Watt, M. J. (2009) Adipose triacylglycerol lipase deletion alters whole body energy metabolism and impairs exercise performance in mice. *Am. J. Physiol. Endocrinol. Metab.* **297,** E505–E513
40. Schoiswohl, G., Schweiger, M., Schreiber, R., Gorkiewicz, G., Preiss-Landl, K., Taschler, U., Zierler, K. A., Radner, F. P., Eichmann, T. O., Kienesberger, P. C., Eder, S., Lass, A., Haemmerle, G., Alsted, T. J., Kiens, B., Hoefler, G., Zechner, R., and Zimmermann, R. (2010) Adipose triglyceride lipase plays a key role in the supply of the working muscle with fatty acids. *J. Lipid Res.* **51,** 490–499